Supermode analysis of Ring waveguide

JOÃO PAULO N. TORRES[a,*], VICTOR MALÓ MACHADO[a], ANTÓNIO BAPTISTA[b]
[a]*Instituto de Telecomunicações, Instituto Superior Técnico, Univesidade de Lisboa, Lisboa, Portugal*
[b]*Instituto Superior Técnico, Univesidade de Lisboa, Lisboa, Portugal*

Propagation supermodes have been analysed in concentric ring waveguides. The ring waveguide core is divided into three layers each one with a constant refractive index. The influence of the central layer width in the electrical field propagation is analysed as a function of the waveguide refractive index.

(Received September 30, 2015; accepted August 9, 2017)

Keywords: Ring, Waveguide, Layer

1. Introduction

Ring lasers have been used in several optical devices such as amplifiers [1], filters [2], logical elements [3], multiplexers / desmultiplexers [4] and sensors [5].

They are important building blocks for photonic devices in optical integrated circuits [6,7]. Numerous scientific works have been published on the analytical analysis of linear dielectric ring lasers with a constant refractive index inside the cavity [8,9].

The device fabrication with the inclusion of ring lasers is the most promising and sustainable element in the manufacture of optical and electro-optical integrated circuits, with a high density of integration (VLSI).

In the nonlinear optical domain, ring lasers have also importance. Initially, the structures were cumbersome and large. The solution to this problem appears with the rise of the integrated optics. The first semiconductor ring laser was demonstrated in the 80's [10,11].

In the last years, ring semiconductor laser with a circular geometry has been studied, since they do not need mirrors to ensure light feedback. The lasers and other devices based on ring structures has been adopted as the basic devices in the design of optoelectronic integrated circuits. These devices have applications in the generation of ultra-short pulses, rotation sensors, digital circuits and digital optical memories [12-16].

Due to the importance of the ring lasers structures, in this paper the electrical field propagation is studied in this type of structures.

In the present work, a model based on an analytical approach is used to describe the TE supermodes propagation in 2-D ring lasers waveguides.

This model could be extended to other devices namely diode lasers with ring resonators [17, 18] where nonlinear optical effects are present. In these cases, modal properties of the ring waveguides are dependent on the nonlinear variation of the media refractive index with the electric field. In some problems, the perturbation theory [19] can be used allowing an analytical approach. In problems with higher geometrical complexity, numerical techniques, such as the finite element method (FEM) [20, 21], should be applied.

The paper is organized according the following section: in section II the propagation model is present; in section III some results will be discussed and in section IV some conclusions are presented. The simulation processes and the corresponding software was developed by the authors.

2. Propagation model

In Fig. 1 the structure studied in this paper is shown.

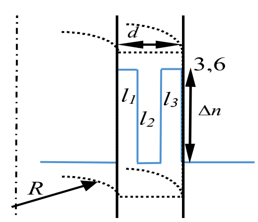

Fig. 1. Waveguide transversal section. The blue line is the refractive index profile, d is the total waveguide width, l_1, l_2, l_3 are the three waveguide layer widths (l_1+l_3=d-l_2) and R is the curvature radius

The material properties remain constant in the azimuthal coordinate, considered as the propagation direction, allowing the use of a 2D approach model to the electric field propagation. It is also considered that the waveguide core is divided into three layers.

Similarly to [22] and [23, 24], Bessel functions have been used to describe the electric field propagation into the waveguide. The electromagnetic field is achieved from the space-time Maxwell equations:

$$\nabla \times \mathbf{E} = -\frac{\partial \mathbf{B}}{\partial t} \tag{1}$$

$$\nabla \times \mathbf{H} = \mathbf{J} + \frac{\partial \mathbf{D}}{\partial t} \quad (2)$$

$$\nabla \cdot \mathbf{D} = \rho \quad (3)$$

$$\nabla \cdot \mathbf{B} = 0 \quad (4)$$

$\mathbf{D}=\varepsilon\mathbf{E}$ and $\mathbf{B}=\mu\mathbf{H}$ are the medium constitutive equations. The medium is considered linear and isotropic, without dielectric or magnetic losses. The vector **D** is the electric displacement, **E** the electric field strength, **B** the magnetic induction vector, **H** the magnetic field intensity, **J** the electric current density and ρ the electric charge density. It is supposed that there is no electrical charges and electric current distributions inside the waveguide. The electric field is calculated assuming an harmonic variation on time ($e^{j\omega t}$, ω is the angular frequency). With these assumptions the Maxwell's equations in the frequency domain take the following form:

$$\nabla \times \mathbf{E} = -j\omega\mu\mathbf{H} \quad (5)$$

$$\nabla \times \mathbf{H} = j\omega\varepsilon\mathbf{E} \quad (6)$$

$$\nabla \cdot \mathbf{E} = 0 \quad (7)$$

$$\nabla \cdot \mathbf{H} = 0 \quad (8)$$

The electric and magnetic fields in ring waveguides are described by:

$$\mathbf{E}(r,\theta,z,t) = (E_r, E_z, E_\theta)(r,z)e^{j(\omega t - \nu\theta)} \quad (9)$$

$$\mathbf{H}(r,\theta,z,t) = (H_r, H_z, H_\theta)(r,z)\, e^{j(\omega t - \nu\theta)} \quad (10)$$

where ν is the propagation constant.

Due to the existence of energy losses by radiation, the complex propagation constant is defined as: ν = β-jα, β > 0, α > 0. The real part is the phase constant and the imaginary part the attenuation constant.

In this paper, it is analyzed the TE^z modes. With $E_z = \phi$ and $E_r = 0$ the following equations will be obtained:

$$H_r = \frac{1}{j\mu_0\omega}\left[j\frac{\nu}{r}\phi + \frac{\partial E_\theta}{\partial z} \right] \quad (11)$$

$$H_\theta = \frac{1}{j\mu_0\omega}\frac{\partial \phi}{\partial r} \quad (12)$$

$$E_\theta = -j\frac{1}{\nu}r\frac{\partial \phi}{\partial z} \quad (13)$$

$$\frac{1}{rj\mu_0\omega}\frac{\partial}{\partial r}\left(r\frac{\partial \phi}{\partial r} \right) + \frac{j\nu}{r}\left(\frac{1}{j\mu_0\omega}\left[j\frac{\nu}{r}\phi + \frac{\partial E_\theta}{\partial z} \right] \right) = jn^2\varepsilon_0\omega\phi \quad (14)$$

where *n* is the refractive index. With some simplification, it is possible to find the wave equation:

$$\nabla^2\phi - \frac{\nu^2}{r^2}\phi + n^2k_0^2\phi = 0 \quad (15)$$

where $k_0 = \omega/c_0 = 2\pi/\lambda$ is the wave number, c_0 the speed of light and λ the wavelength.

Equation (15) admits the particular solution:

$$\begin{cases} F''(z) + k_z^2\, F(z) = 0 \\ T''(r) + \dfrac{1}{r}T'(r) + \left(n^2k_0^2 - \dfrac{\nu^2}{r^2} \right)T(r) = 0 \end{cases} \quad (16)$$

where k_z is the propagation constant along the *z* direction.

Due to the symmetric properties of the system, the electromagnetic field remains constant in the axial direction (z).

The second equation is a Bessel differential equation with the Bessel functions as a solution:

$$T(r) = \begin{cases} A_s J_\nu(k_s r), & 0 < r < R \\ A_i J_\nu(k_i r) + B_i Y_\nu(k_i r), & R < r < R + d \\ A_c H_\nu^{(2)}(k_c r), & r > R + d \end{cases} \quad (17)$$

In the waveguide, when *r*→0, the solution denoted by index *s* is the Bessel function of first kind. For the waveguide core, where an index *i* is used, the solution is a combination of first and second kind Bessel functions and for the outer region (*r*→∞) - index *c* - the solution is a Hankel function of the second kind. All the Bessel functions have order ν and argument *kr*, where ν is the complex propagation constant and *k* is given by nk_0, *n* being the refractive index of the corresponding layer.

The coefficients *A* and *B* are acquired by the boundary conditions to assure the continuity of ϕ and $\partial\phi/\partial r$ at the discontinuity interfaces.

In the eigenvalue problem, describe by eq. 17, the eigenfunction is associated with the electric field and the eigenvalue is associated with the propagation constant.

The boundary conditions at each interface result in a 2 (N + 1) system of homogeneous equations. All the constants should be determined except one of them which is imposed. The elimination of these coefficients results in the determination of an equation for the propagation constant ν.

The electric field profile is normalized using energy considerations involving the active power, related to the real part of the Poynting vector: $\mathbf{S}_{av} = \frac{1}{2}\Re\left[\mathbf{E}\times\mathbf{H}^*\right]$.

For ring waveguides, the radial and azimuthal components of $\mathbf{S}_{av}$ are given by:

$$S_{av,r} = -\frac{1}{2\mu_0\omega}\Re\left[jE_z\frac{\partial E_z}{\partial r} \right]e^{-2\alpha\theta} \quad (18)$$

$$S_{av,\theta} = \frac{\beta}{2\mu_0\omega}\frac{1}{r}\left|E_z\right|^2 e^{-2\alpha\theta} \tag{19}$$

The total energy flux along the azimuthal direction per unit axial length and time is determined as:

$$P_\theta(\theta) = \int_0^\infty S_{av,\theta}dr = \frac{\beta}{2\mu_0\omega}e^{-2\alpha\theta}\int_0^\infty \frac{\left|E_z\right|^2}{r}dr \tag{20}$$

In order to achieve an arbitrary unit (a.u.) to the electric field, the following quantity is used as the normalization constant:

$$\sqrt{\mu_0\omega P_\theta(\theta)} \tag{21}$$

In all simulations the excitation source is located in θ=0, where the complex amplitude module of the field is maximum.

3. Results

In this section, some results are analyzed for the waveguide shown in Fig. 1.

In this structure, the waveguide core is divided into three layers. The central layer (l_2) and the waveguide external region have the same refractive index. The other two layers (l_1 and l_3) have a refractive index equal to 3.6. The simulation is performed using a waveguide radius of R= 50 µm and fixed l_1 =l_3=0.5µm.

The effect of the refractive index difference Δn between the layers l_1 ,l_3 and the central layer l_2 for several l_2 width values is analyzed imposing a wavelength λ = 0.8 µm. Fig. 2 shows the fundamental supermode profiles of the electric field for two situations: one for Δn = 0.15 (Fig. 2 a)) and another for Δn = 0.3 (Fig. 2 b)).

As the width l_2 increases, the position of the electric field maximum value starts to be shifted to the layer l_3. This effect is quite different from the case of straight waveguides with the core split in three layers too. In this case, the field is described by a symmetric curve centered in the middle of the l_2 layer. The asymmetric distribution of the electric field, observed in our case, is directly related to the mechanism of curvature losses.

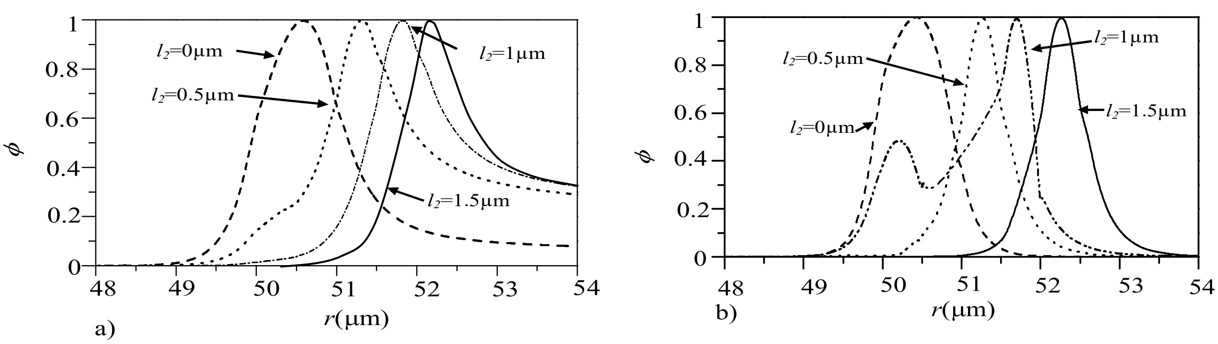

Fig. 2. Fundamental mode profile of the electrical field as a function of the layer width l_2 for two Δn: a) for Δn =0.15 and b) for Δn=0.30

With a cautious examination of Fig. 2 b), it is possible to identify a particular case for l_2= 1 µm. The electric field confinement mechanism allows the understanding of this situation. The electric field not only is confined into the layer l_3 but also starts to be confined into the layer l_1(maximum located in l_1). However, the majority of the electric filed is located in layer l_3. For the same situation, but for the smaller value of Δn (Fig. 2 a)) the electric field is almost completed located in layer l_3. In this case the mechanism of curvature losses are much higher since Δn is much smaller than in the previous case.

The mechanism of energy transfers between l_1 and l_3 and in the opposite direction is not equal since the electric field is scattered in a non-symmetric way between layers l_1 and l_3.

In Fig. 3 the real and the imaginary part of the propagation constant, which are the phase constant and the attenuation constant, respectively, are represented as a function of the width l_2 for several Δn values.

The phase and attenuations constants when Δn < 0.2 increase with the increase of l_2.

As the refractive index difference increase and the electric field confinement is increased and becomes dominant, some non-linear behaviors in the phase and attenuation constant for specifics l_2 width values appear as a consequence of the matching of the two referred mechanisms: the electric field confinement and the curvature losses.

An inspection of the curve corresponding to Δn=0.4 (solid curve) shows the existence of two minimums in the phase constant set around λ and λ/2.

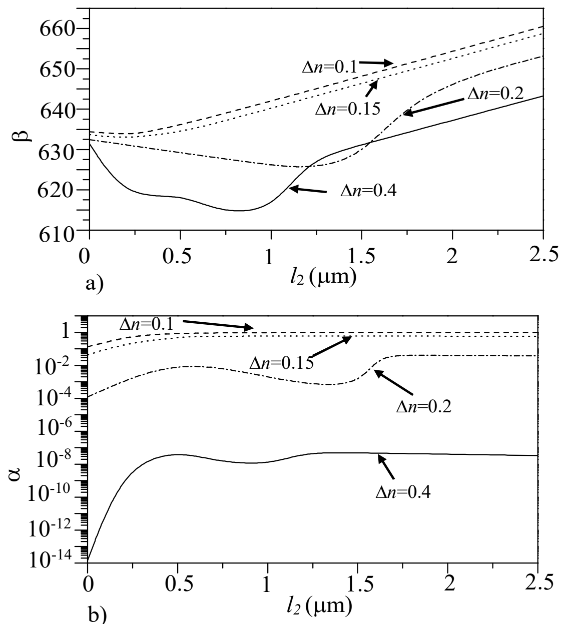

Fig. 3. Propagation constant as a function of the l_2 width for different Δn values. In fig a) is shown the real component of the propagation constant and in fig. b) the imaginary component of the propagation constant

Thus, for l_2 multiples of the subwavelength some effects arise that lead to a non-monotonic behavior in the progress of the phase constant. As already mentioned, this effect is only visible for $\Delta n > 0.2$, supporting the idea that the influence of layer l_1 is only relevant for higher values of Δn.

4. Conclusion

In the previous results, it was analyzed the electric field profile of the fundamental supermode, in ring waveguides. In all the results, the waveguide core was split into three layers, each one with a constant refractive index.

In this type of structures, two mechanisms must be considered: the electric field confinement and the curvature losses. It may be concluded that when the confinement is the dominant mechanism a non-linear behavior appears in the results.

Acknowledgments

This work was supported by national founds through the Fundação para a Ciência e a Tecnologia (FCT) of the Portuguese Government with reference UID/EEA/50008/2013.

References

[1] D. Hall, P. Jackson," The Physics and Technology of Laser Resonators", Taylor Francis, 1989.

[2] V. Bykov, O. Silichev, "Laser Resonators" Cambridge International Science Publishing, 1995.

[3] A. Kudryashov, H. Weber, "Laser Resonators: Novel Design and Development" SPIE Optical Engineering Press, 1999.

[4] N. Hodgson, H. Weber, "Laser Resonators and Beam Propagation", Springer 2005.

[5] S. K. Dixit, "Filtering Resonators", Nova Science Publishers 2001.

[6] B. E. Little, S. T. Chu, H. A. Haus, J. Foresi, J.-P. Laine, IEEE Journal of Lightwave Technology **15**, 998 (1997).

[7] M. Bertolotti, A. Driessen, F. Michelotti, editors. Microresonators as building blocks for VLSI photonics, **709** of AIP Conference Proceedings. American Institute of Physics, Melville, New York, 2004.

[8] E. A. J. Marcatili, Bell Syst. Tech. J. **48**(7), 2103 (1969).

[9] D. Marcuse, Bell Syst. Tech. J. **50**(8), 2551 (1971).

[10] A. S. Liao, S. Wang, Applied Physics Letters **36**(10), 801 (1980).

[11] H. Cao, C. Liu. H. Deng, M. Benavidez, V. Smagley, R. Caldwell, G. Peake, G. Smolyakov, P. Eliseev, M. Osinski, Applied Physics Letters **86**(4), 041101 (2005).

[12] J. J. Liang, S. T. Lau, M. H. Leary, J. M. Ballantyne, Applied Physics Letters **70**(10), 1192 (1997).

[13] Y. Liu, T. Hill, N. Callabretta, H. de Waardt, G. D. Khoe, H. Dorren, IEEE Photonics Technology Letters **15**(10), 1461 (2003).

[14] E. Bente, Y. Barbarin, J. den Besten, M. Smit, J. Binsma, IEEE Journal of Quantum Electronics **40**(9), 1208 (2004).

[15] R. Grover, P. P. Absil, T. A. Ibrahim, P.-T. Ho, Ettore Majorana Centre for Scientific Culture, International School on Quantum Electronics, Sicily, Italy, 18 (2003).

[16] Zhuoran Wang, Guy Verschaffelt, Yi Shu, Gabor Mezozi, Marc Sorel, Jan Danckaert, Siyuan Yu, IEEE Photonics Letters **20**(2), 99 (2008).

[17] T. Kraus, P. J. R. Laybourn, J. Roberts, Electron. Lett. **26**(25), 2095 (1990).

[18] S. L. McCall, A. F. J. Levi, R. E. Slusher, S. E. Pearton, R. A. Logan, Appl. Phys. Lett. **60**(3), 289 (1992).

[19] Arun Kumar, Deepak Gupta, Optics Communications **274**(2), 327 (2007).

[20] Z. Jovanoski, I. N. Towers, N. A. Ansari, R. A. Sammut, Optics Communications **244**, 399 (2005).

[21] B. M. Azizur Rahman, J. Brian Davies, IEEE Trans. Mricrowave Theory Tech. **MTT-32**(1), 20 (1984).

[22] K. R. Hiremath, M. Hammer, R. Stoffer, L. Prkna, J. Ctyroky, Optical and Quantum Electronics **37**(1-2), 37 (2005).

[23] C. Vassallo "Optical Waveguide Concepts" Elsevier, 1991.

[24] J. Torres, A. Baptista, V. M. Machado, Journal of Lightwave Technology **31**(13), 2140 (2013).

*Corresponding author: joaotorres@ist.utl.pt